Analysis of out-of-plane performance of composite slab with precast concrete ribbed panels under a hanging load

Jingshu Zhang, Binyang Liu, Binbin Han, Yongsong Ni, and Zhenlong Li

■ Full-scale static hanging load tests of a two-way, two-span composite slab with precast concrete ribbed panels and a cast-in-place concrete slab were conducted, and the out-of-plane deflections and crack resistance of the two systems were compared.

■ The stiffness and crack resistance behavior of the composite slab was similar to that of the cast-in-place concrete slab, but the composite slab could support more load at the maximum crack control limit.

■ Additional analysis of the composite slab showed that the precast concrete ribbed panels provide more shear strength on the combined interface than typical flat-plate composite slabs provide.

In the 1920s, composite slabs consisting of precast concrete panels with a composite cast-in-place concrete topping were used to bridge construction, and in the 1940s, these slabs were used in residential construction. Composite slabs were developed to solve problems associated with prefabricated concrete structures, such as a lot of crane work, and those with cast-in-place concrete structures, such as long construction periods and the use of formwork and falsework.[1,2]

The composite action between precast concrete panels and the cast-in-place concrete topping has been the subject of many research projects in various construction applications. The experimental studies of Baran[3] and Scott[4] have shown that hollow-core slabs with a concrete topping maintain good composite action and can meet the requirements for shear and bending under service loads. Adawi et al.[5] conducted full-scale tests of five hollow-core slabs using three-point bending, and the results showed that a roughened surface between the precast and cast-in-place concrete elements with an amplitude greater than 0.3 mm (0.012 in.) could provide sufficient shear strength up to the ultimate bearing capacity. Kumar and Ramirez[6] studied the effect of shear connectors and varying the applied prestress on the mechanical properties of composite decks with precast concrete panels. The study found that the combined interface (which was broom swept only) could meet the requirements for shear strength if the nominal average horizontal shear stress at the interface was less than 0.8 MPa (116 psi). Tang et al.[7] and Li et al.[8] tested steel bar truss and concrete superimposed slabs. Their experimental study indicated that the

precast concrete and steel bar truss panel and the cast-in-place portion of the composite slab performed well, but the stiffness and crack resistance of the two-way superimposed slabs were slightly lower than those of an all cast-in-place concrete slab. An et al.[9] conducted experimental research on the mechanical performance of two-way prestressed laminated concrete slabs under uniform load. The study proposed joint details that transferred the steel reinforcing bar force continuously through the slab joints to improve the integrity of the two-way prestressed laminated concrete slabs.

The aforementioned studies considered several types of composite slabs and a variety of issues regarding the mechanical performance of composite slabs; however, several key aspects of composite slab behavior remain to be investigated:

• In the experimental setups of previous studies,[3–6] it was difficult to observe cracks on the upper surface of the specimens during tests and the tests did not reflect the overall performance of the composite slabs under the least favorable conditions (which is when there is tensile stress on the combined interface) because the loading was on the top slab surface. Moreover, loading the top slab surface improves the performance of the composite slabs because the pressure on the upper surface increased the shear friction on the combined interface.

• The end supports for the specimens in previous studies[3–6] were usually hinged, which does not represent actual boundary conditions (fixed supports) that are typically used in construction.

• The specimens for previous tests[3–6] were usually a single component (consisting of a single precast concrete panel with a composite cast-in-place topping) that has a different behavior compared with the full-scale composite slabs (consisting of several precast concrete panels and a composite cast-in-place topping) that are typically used in construction.
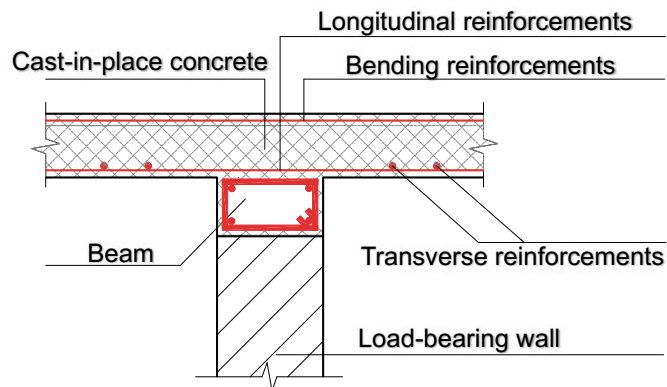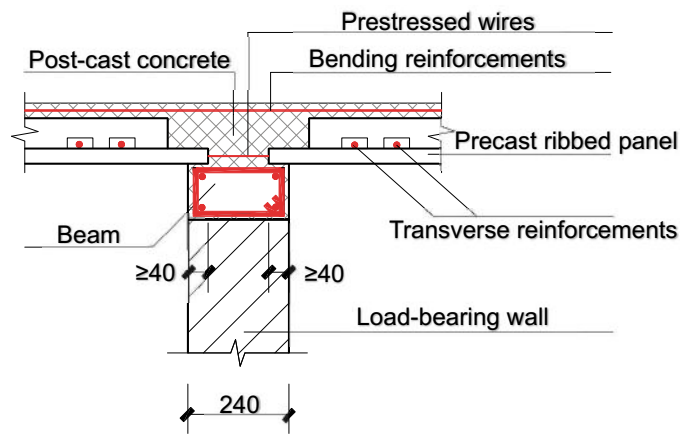
A composite slab with precast concrete ribbed panels (CSPRP) is a new type of composite slab consisting of precast concrete panels with ribs that have regularly distributed rectangular holes[10,11] and a cast-in-place concrete topping (**Fig. 1**). The ribs of the precast concrete panel and the cast-in-place concrete that fills the rectangular holes of the ribs act as a shear key and provide an interlocking mechanism that increases the integrity and shear capacity at the combined interface of the CSPRP.[12–14] By loading the top surface of the CSPRP, Wu et al.[15] studied the out-of-plane performance of a CSPRP that was simply supported on four sides and subjected to uniformly distributed loads. The results showed that prestressing increased the cracking load of the CSPRP and reduced its ductility. Moreover, the CSPRP exhibited typical crack distribution and yield failure mode. Yao et al.[16] analyzed the cost of the CSPRP, and the results showed that CSPRP has obvious economic benefits: its cost was about 95% that of cast-in-place slab and was only 41% that of a combination floor with a corrugated steel deck.
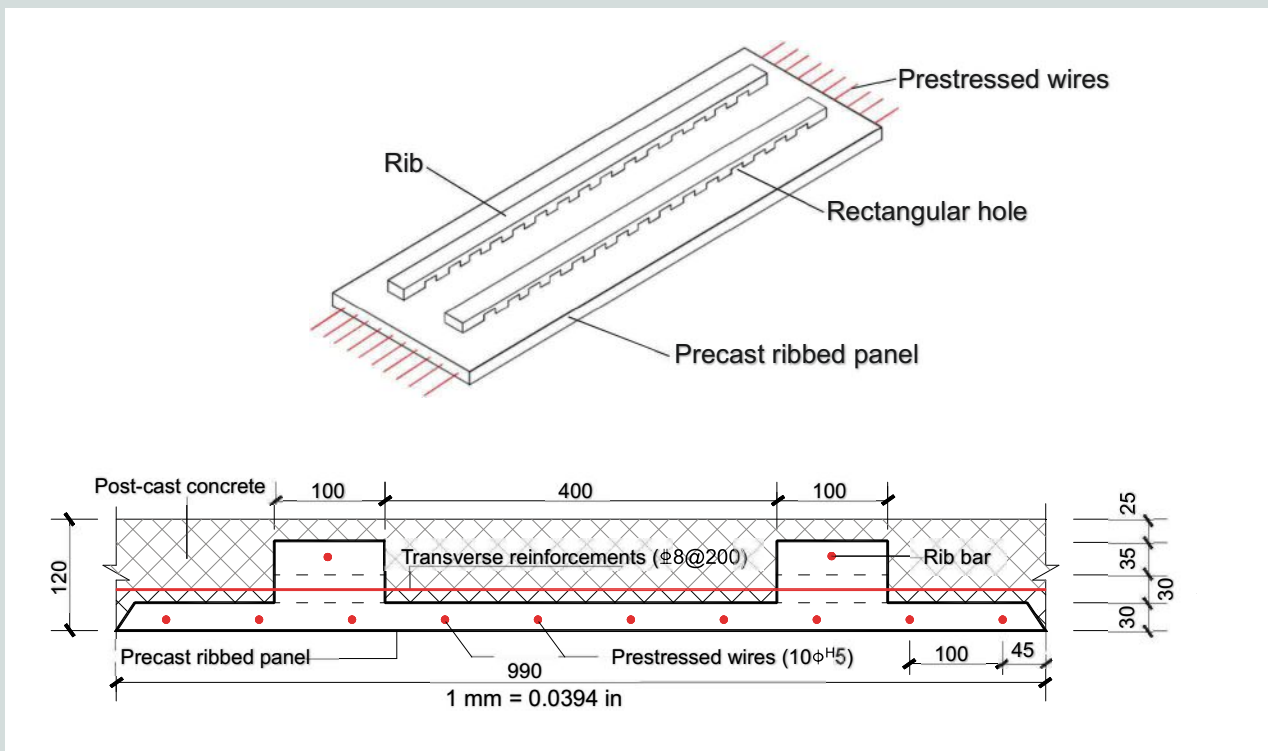
Figure 1. Precast concrete ribbed panel. Note: All dimensions are in millimeters. 1 mm = 0.03937 in.

Figure 2 is a full-page figure with three schematic diagrams.
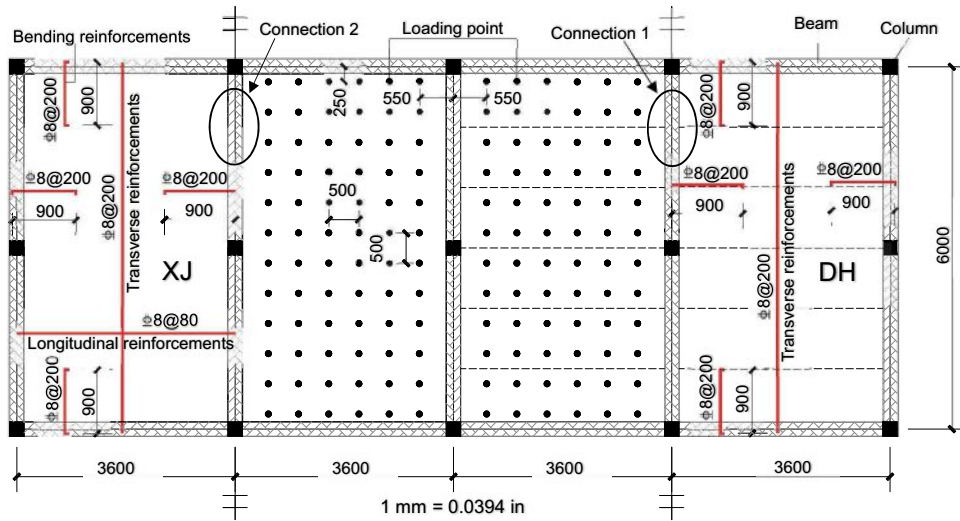
Plan view of the CSPRP and
cast-in-place concrete slab

Connection 1

Connection 2

Figure 2. Reinforcement details of the CSPRP and cast-in-place concrete slab and the loading-point layout schematic. Note: All dimensions are in millimeters. CSPRP = composite slab with precast concrete ribbed panels. 1 mm = 0.03937 in.

When there is a change of use of an existing building, some equipment, pipes, or other items may be hung under the floor by means of expansion bolts anchored into the floor. In these cases, the combined interface of the composite slabs will be subjected to combined tensile and shear stresses, which is more critical than loading the top surface of the slab. This paper examines the out-of-plane performance of CSPRPs under this more-critical condition. A static hanging load test of a two-span, two-way CSPRP was conducted in which the load was placed on a loading frame and suspended from the ribs of the precast concrete ribbed panel (PRP) after the cast-in-place concrete topping reached its design strength. In addition, a separate test of a two-span, two-way cast-in-place concrete slab was conducted under the same conditions to compare the performance of the two systems.

Test program

Specimen details

This experiment was conducted in conjunction with a construction project for a single-story parking structure consisting of four identical compartments. Each compartment had a plane dimension of 3600 × 6000 mm (141.7 × 236.2 in.). The tests were carried out on the roof slab of the parking structure.

The PRPs were reinforced with 5 mm (0.2 in.) diameter prestressed wires spaced at 100 mm (3.94 in.) with an initial prestress of 864 MPa (125 ksi), which is 55% of the standard breaking strength of the wires. Each PRP had a span of 3600 mm (141.7 in.) and width of 1000 mm (39.4 in.) (Fig. 1).

Two two-span, continuous, two-way slabs were produced for this test. One slab was the CSPRP constructed with six PRPs in each span and marked as specimen DH. There were 10 mm (0.40 in.) gaps between each adjacent PRP under construction for ease of assembly. Cast-in-place concrete filled the gaps between PRPs to increase the integrity of the CSPRP. The other slab was a cast-in-place concrete slab used for comparison with the CSPRP and marked as specimen XJ (**Fig. 2**). The cross-section dimensions, concrete strength, bearing condition, and load arrangement for specimens DH and XJ were the same. Each specimen was 3600 × 6000 × 120 mm (141.7 × 236.2 × 4.7 in.). Specimen DH was prestressed in the short-span direction, and the reinforcement of specimen XJ was equivalent to that of specimen DH. The reinforcement of specimens DH and XJ were the same except for the longitudinal reinforcement in the short-span direction. (The longitudinal reinforcement for specimen DH was prestressed wires, while reinforcing bars with a diameter of 8 mm [0.31 in.] were used for specimen XJ.) The spacing of the reinforcing bars along the short-span direction of specimen XJ was calculated to provide reinforcement equivalent to the prestressed wires in specimen DH.

Based on the principle of strength equivalence of steel, the following formula can be obtained:

$$\frac{A_s}{dh}f_{su} = \frac{A_p}{d_1 h}f_{pu} \qquad (1)$$

where

A_s = area of single reinforcing bar used for the longitudinal reinforcement in the short-span direction of specimen XJ

d = spacing of the longitudinal reinforcement in the short-span direction of specimen XJ

h = thickness of specimens XJ and DH

f_{su} = measured average ultimate tensile strength of reinforcing bar used for the longitudinal reinforcement in the short-span direction of specimen XJ

A_p = area of single prestressed wire used for the longitudinal reinforcement in the short-span direction of specimen DH

d_1 = spacing of the prestressed wires of specimen DH

f_{pu} = measured average ultimate tensile strength of prestressed wire used for the longitudinal reinforcement in the short-span direction of specimen DH

After some transformations, Eq. (1) takes the following form:

$$d = \frac{A_s f_{su} d_1}{A_p f_{pu}} \qquad (2)$$

Substituting data into Eq. (2), the calculated value of d was approximately 80.5 mm (3.17 in.), and a reinforcing bar spacing of 80 mm (3.15 in.) was used to construct specimen XJ.

The longitudinal reinforcement and bending reinforcement were continuous over the intermediate support of the two-span, continuous, two-way cast-in-place concrete slab. The bending reinforcement of the two-span, continuous, two-way CSPRP was also continuous over the intermediate support. Before placing the cast-in-place concrete on the PRP, the surface of the PRP was broom swept and fully wetted to ensure that the interface between the PRP and cast-in-place concrete were prepared consistent with typical construction practices.

The physical properties of the concrete and the reinforcement are summarized in **Tables 1** and **2**, respectively. The concrete strength grade in Table 1 is defined according to the Ministry of Housing and Urban-Rural Construction of the People's Republic of China's *Code for Design of Concrete Structures*.[17]

Test method

Previous studies[3,4,6–11,14] of composite slab systems have placed loads on the top surface of the slabs. In these studies, loads are typically applied as either concentrated loading, which

**Table 1.** Measured compressive strength of concrete

Specimen number	f_c of precast concrete ribbed panel, MPa	Concrete strength grade	f_c of cast-in-place concrete, MPa	Concrete strength grade
XJ-1	n/a	n/a	27.1	C40
XJ-2	n/a	n/a	26.9	C40
DH-1	27.3	C40	26.8	C40
DH-2	26.9	C40	27.5	C40

Note: f_c = average value of measured concrete compressive strength; n/a = not applicable. 1 MPa = 0.145 ksi.

Table 2. Measured tensile strength of reinforcement

| Reinforcement type	f_y, MPa	f_u, MPa
Transverse, bending, and longitudinal reinforcement (8 mm diameter)	449.5	560.0
Prestressed wire (5 mm diameter)	n/a	1781.7

Note: f_y = average value of measured yield tensile strength; f_u = average value of measured ultimate tensile strength; n/a = not applicable. 1 mm = 0.03937 in.; 1 MPa = 0.145 ksi.
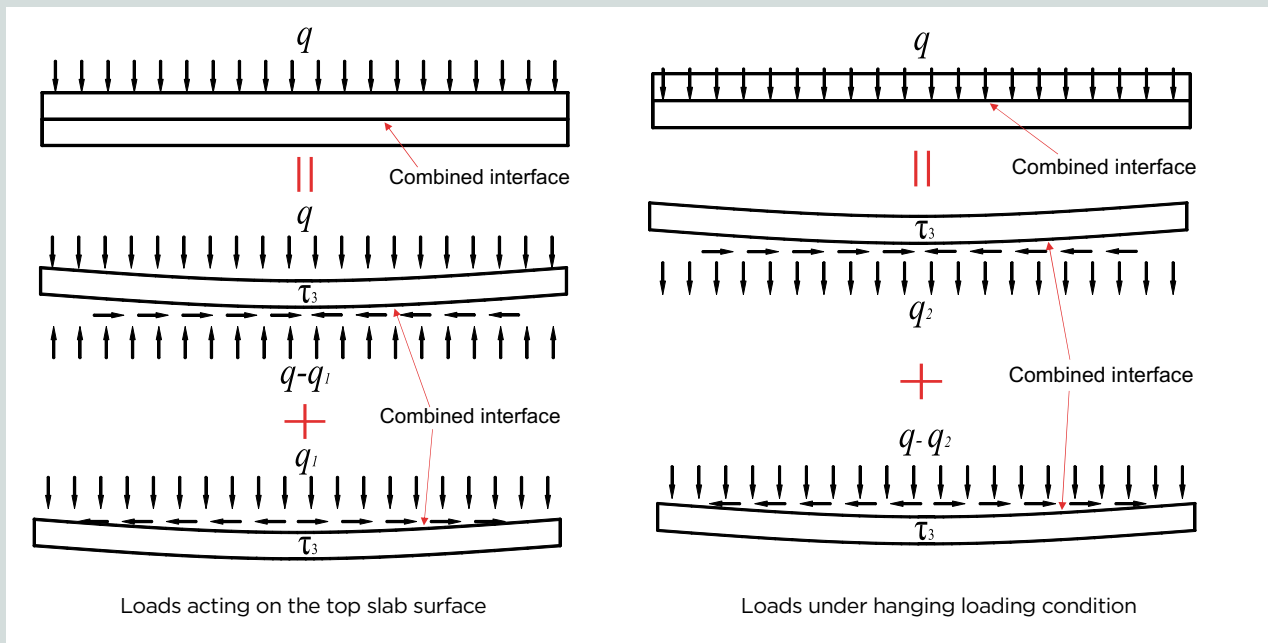
Figure 3. Stress distribution on combined interface under different loading conditions. Note: q = uniform load acting on the plate; q_1 = compressive stress on the combined interface; q_2 = tensile stress on the combined interface; τ_3 = shear stress on the combined interface.

usually adopts single-point loading[3,6,14] or uniform loading.[4,7–11] Uniform loading is usually achieved by laying bricks or sandbags or setting a water tank (with a very soft bottom) on the top surface of the slab. For these types of loading, the load path is from the top to the bottom of the slab. Thus, no tensile stress should occur on the combined interface (**Fig. 3**). However, in building applications, loads may be applied to the bottoms of slabs, such as by connecting suspended ceilings, which produce tensile stresses on the interface of the precast concrete panel and cast-in-place slab. The integrity of the CSPRP is increased and the composite action of the CSPRP is overestimated if the top-loading methods are used. In addition, when bricks, sandbags, or water tanks are placed on the top surface of the slab to apply the load, experimental
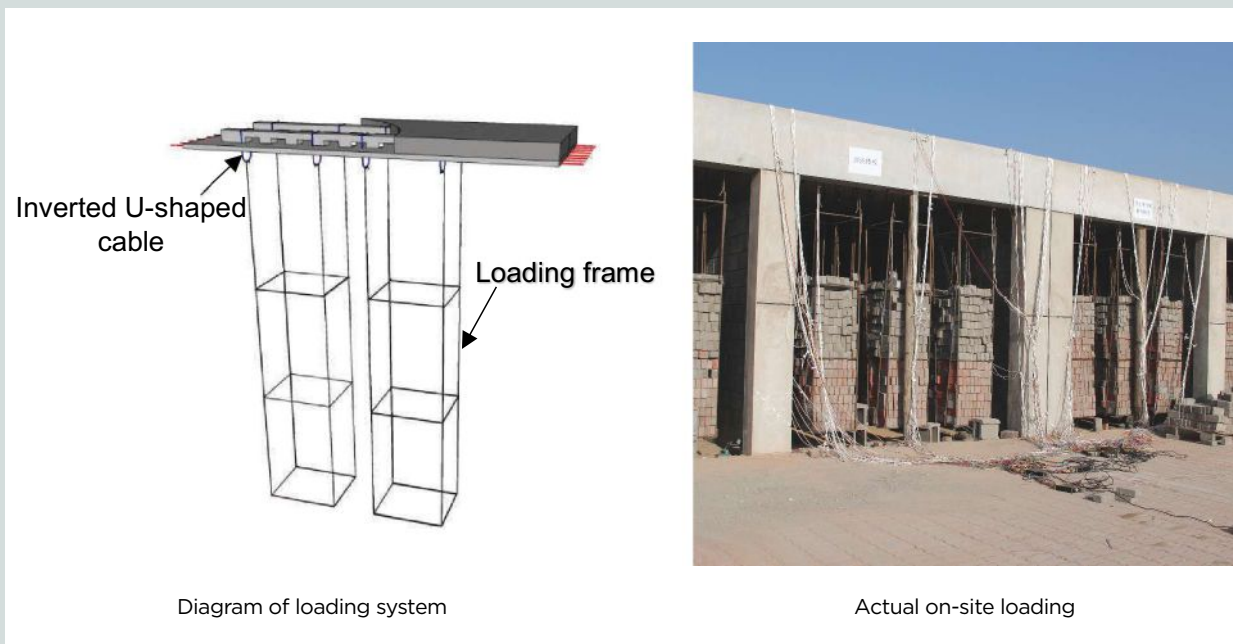
Figure 4. Schematic diagram and photo of the hanging loading method.

observations of the slab under the load are limited. Likewise, the development of cracks on the top surface of the slab under the load cannot be observed and the distribution of cracks can only be clearly seen after unloading.

To apply the hanging load, an inverted U-shaped cable was suspended from the ribs of the PRP at the loading point before placing the cast-in-place concrete topping (**Fig. 4**). The PRP had a 12 mm (0.47 in.) diameter hole drilled near each side of the ribs at the hanging point for the inverted U-shaped cable to pass through. The transverse and bending reinforcement were placed on the PRP, and the cast-in-place concrete topping was placed. After the cast-in-place concrete topping achieved its design strength, concrete blocks were stacked in the loading frame to load the slabs. Specimen XJ was loaded in the same way as specimen DH. Each loading frame was suspended at four loading points, with vertical loading points spaced 500 mm (19.7 in.) apart and 72 load points distributed evenly along each span (Fig. 2). This loading point distribution is sufficiently dense to approximate uniform loading on the slab.

Compared with the traditional method of loading on the top surface of the slab, the combined interface of the CSPRP is affected by shear stress and tensile stress (Fig. 3) under a hanging load. Therefore, the stress on the combined interface is greater when using a hanging load compared with the traditional loading method, and thus it is more effective for testing the out-of-plane performance of the CSPRP under extreme stress conditions. In addition, because the loads are placed in the loading frame when the hanging load is applied, crack development can be observed on both the top and bottom slab surfaces during testing.

To obtain the out-of-plane deflection of the specimens, measuring points were placed at the midspan of each specimen (**Fig. 5**).

Loading system

The design load for the specimens was 10 kN/m² (1.45 psi) under normal service conditions. According to the China Academy of Building Research's *Standard Method for Testing of Concrete Structure*,[18] the incremental step load should be 0.2×10 kN/m², which is equal to 2 kN/m² (0.2×1.45 psi = 0.29 psi). For simplicity, the test was conducted using concrete blocks. **Table 3** shows the actual increment step load used for testing. During formal testing, the load was maintained for
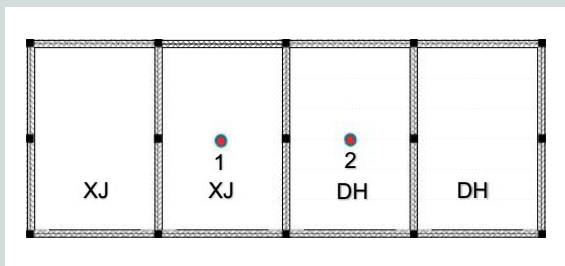
Figure 5. Measuring point arrangement. Note: 1 = location for out-of-plane deflection measurement for specimen XJ; 2 = location for out-of-plane deflection measurement for specimen DH.

Table 3. Loading system

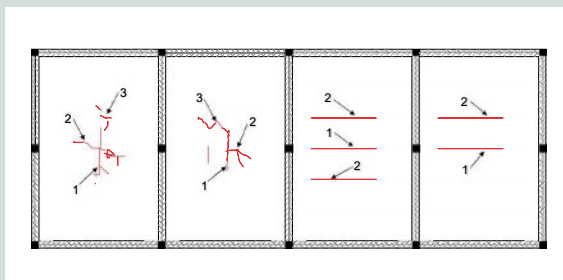| Load stage	Cumulative layers of concrete blocks	Load of each stage, kN/m²	Cumulative load, kN/m²	Remarks
1	4	2.76	2.76	n/a
2	8	2.76	5.52	n/a
3	12	2.76	8.28	Cracks were observed in specimens DH and XJ
4	15	2.07	10.35	n/a
5	17	1.38	11.73	Loading of specimen XJ was stopped
6	19	1.38	13.11	n/a
7	21	1.38	14.49	Loading of specimen DH was stopped

Note: n/a = not applicable. 1 kN/m² = 0.145 psi.

about 10 minutes at each stage. The average weight of 20 concrete blocks that were weighed before the experiment was used to calculate the loading values. When the crack width exceeded 0.1 mm (0.004 in.) or long cracks appeared, the loading was stopped to preserve the specimens for future use.
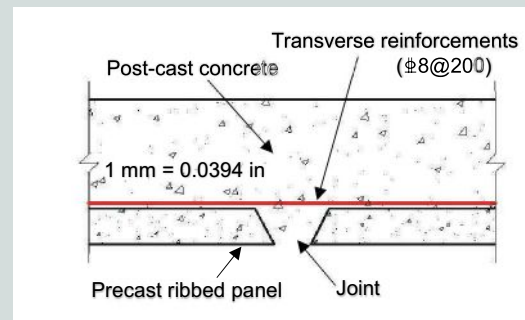
Test results and analysis

Crack distribution

Figure 6 shows the distribution of cracks on the bottom of specimen XJ. When load increased to the third-stage load of 8.28 kN/m² (1.2 psi), crack 1 was observed at the midspan perpendicular to the short span. As the load continued to increase, crack 2, which appeared perpendicular to the long span, and an oblique crack 3, which extended from the center of the slab toward the corner, were observed at the same time. At a load of 11.73 kN/m² (1.7 psi), the length of cracks increased and the loading was stopped to preserve specimen XJ for the parking structure roof. The distribution of cracks showed that specimen XJ exhibited typical two-way stress behavior, and the measured maximum crack width was 0.1 mm (0.004 in.) after loading.
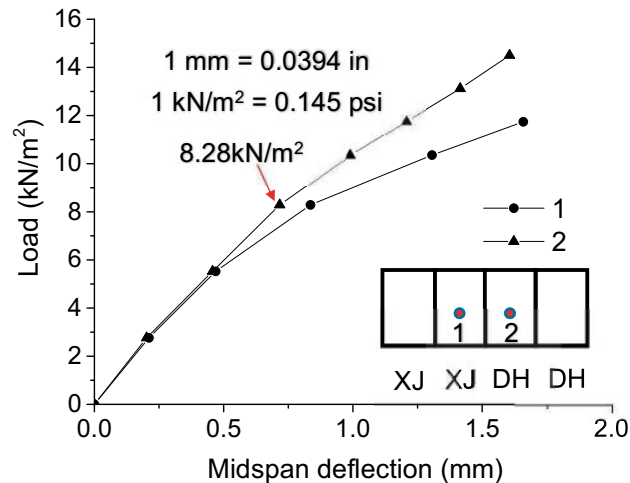
Figure 6 also shows the crack distribution at the bottom of the slab for specimen DH, which exhibited different cracking characteristics from specimen XJ. When loading to the third-stage load of 8.28 kN/m² (1.2 psi), crack 1 appeared at the joint in the middle of the long span. Although the bond strength at the joint of the precast and cast-in-place concrete was small (**Fig. 7**), the joints spanned the direction of the secondary stress of specimen DH (short-span direction was the main force direction). Because the joints in specimen DH were spanning the secondary load direction, the tensile stress at the joint was lower than the stress at the same position of specimen XJ.

Specimen XJ had a non-negligible tensile stress at the bottom of the slab under self-weight, and there was no tensile stress at the joints of specimen DH under self-weight. As a result, specimen DH had an equal cracking load to specimen XJ and both specimens showed considerable resistance to cracking. As the load continued to increase, crack 2 appeared at the adjacent joints on specimen DH and gradually extended along the joints, but a significant increase in crack width was not observed. The transverse reinforcement likely suppressed

Figure 6. Distribution of cracks in the specimens. Note: The numbers in the figure represent the crack numbers described in the text.

Figure 7. Structural detail of joints. Note: 1 mm = 0.03937 in.

Figure 8. Load compared with midspan deflection for specimens DH and XJ. Note: 1 = out-of-plane deflection measurement for specimen XJ; 2 = out-of-plane deflection measurement for specimen DH. 1 mm = 0.03937 in.; 1 kN/m² = 0.145 psi.

the development of cracks along the height of the joints and restricted the crack width. When loading increased to 14.49 kN/m² (2.1 psi), the crack width reached 0.1 mm (0.004 in.). At this load level, the height of the concrete blocks used for loading was 1.9 m (6.2 ft) (Fig. 4). The loading was stopped to preserve specimen DH for the parking structure roof. The load on specimen DH was higher than that of specimen XJ when loading was stopped, but no cracks were observed in the prestressed direction because the prestress increased specimen DH's resistance to cracking. During the entire loading process, no cracks were found at the top surface of specimens DH or XJ.

Load compared with midspan deflection

Figure 8 shows the load compared with midspan deflection for specimens DH and XJ. At the initial stage of loading, the deflection of specimens XJ and DH were similar, increasing almost linearly. This similarity indicated that there was little difference in stiffness between specimens XJ and DH. When loading proceeded to the third-stage load of 8.28 kN/m² (1.2 psi), the slope of the load to midspan deflection curves of the specimens decreased because local cracks appeared at midspan, which resulted in stiffness degradation of the specimens. Specimen XJ exhibited some stiffness degradation before the load reached the cracking load of 8.28 kN/m². This can be attributed to microcracks in the tension zone that existed before the visible cracks appeared. Specimen DH deflected less than specimen XJ at higher loads, probably because specimen DH was cracked only in the nonprestressed direction, which reduced stiffness degradation. The development of midspan deflection in specimens DH and XJ was similar when considering the entire load–to–midspan deflection curve, and although some differences existed after cracking, the results show that specimens DH and XJ exhibited comparable performance.

Overall performance analysis of CSPRPs

This section compares and analyzes the overall performance of CSPRPs and typical flat-plate composite slabs.

Shear strength of the combined interface The possible shear surfaces for CSPRPs and common flat-plate composite slabs are shown in **Fig. 9**. For common flat-plate composite slabs, the theoretical weak shear surface is a plane (the interface between the bottom panel and the cast-in-place concrete topping). Conversely, the CSPRP is a type of ortho-tropic slab and some differences in mechanical properties exist between the different directions. Depending on the direction of the shear force, there are two possible weak shear surfaces for the ribs. Shear surface 1 is along the upper surface of the bottom panel, including the surface around the ribs. Shear surface 2 is along the upper surface of the bottom panel without considering the height of the ribs (because, in this case, shear passes through the ribs). When the shear direction is not parallel to the ribs, the weak shear surface is shear surface 2 because in this case, the shear force cannot cross the interface without proceeding through the ribs (the ribs would be cut). Both shear surface 1 and shear surface 2 have a bonding interface between the cast-in-place and precast concrete and a normal concrete shear surface. (The cast-in-place concrete through the rectangular hole of the ribs is cut in shear surface 1 and the ribs are cut in shear surface 2.)

The average shear strength of the combined interface can be estimated by Eq. (3), and the calculated results are shown in **Table 4**:
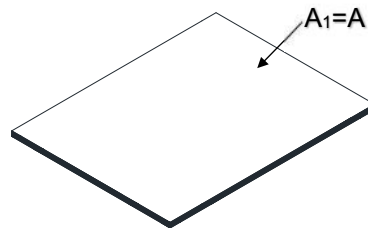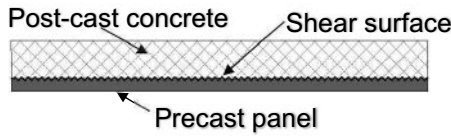
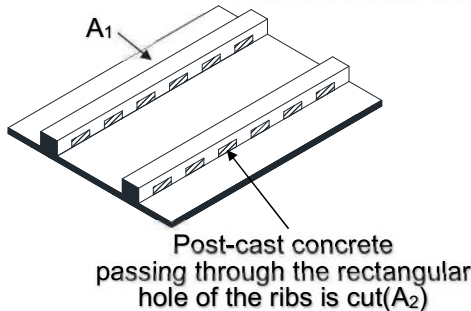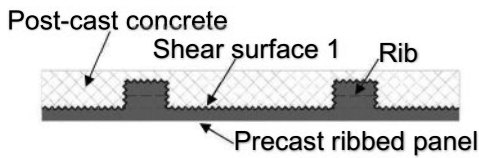$$\tau = \frac{\tau_1 A_1 + \tau_2 A_2}{A} \quad (3)$$

where
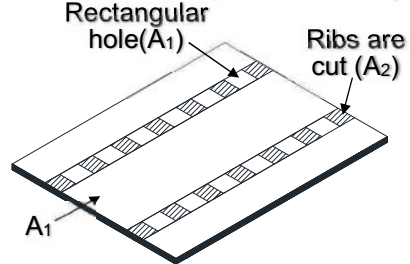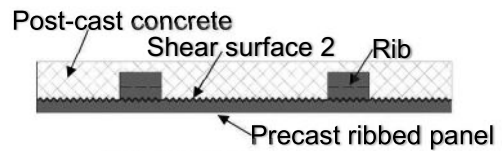
Figure 9. Schematic diagram of the shear surface. Note: A = horizontal projection area of the shear surface; A_1 = area of bonded surface between the cast-in-place and precast concrete on the shear surface; A_2 = area of the normal concrete shear surface (the area where the cast-in-place concrete passing through the rectangular hole of the ribs is cut for shear surface 1 or the area where the ribs are cut for shear surface 2); CSPRP = composite slab with precast concrete ribbed panels.

Table 4. Shear strength and shear strength requirement on combined interface

Types	Shear strength of bond between cast-in-place and precast concrete, MPa	Shear strength of concrete, MPa	Average shear strength of the combined interface calculated by Eq. (3), MPa	Shear stress demand of the combined interface, MPa
CSPRP	0.80	2.39	1.11* (0.94†)	≤0.40
Common flat-plate composite slab	0.80	n/a	0.80	≤0.40

Note: CSPRP = composite slab with precast concrete ribbed panels; n/a = not applicable. 1 MPa = 0.145 ksi.
* Shear surface 1 of CSPRP
† Shear surface 2 of CSPRP

τ = average shear strength of the combined interface

τ_1 = shear strength of the bond between the cast-in-place and precast concrete (The shear-strength value of the cast-in-place and precast concrete bonded surface, which was broom swept only, is 0.8 MPa [116 psi], which was adopted in this paper according to the research of Adawi et al.,[5] Kumar and Ramirez,[6] and Guo et al.[19])

A_1 = area of bonded surface between the cast-in-place and precast concrete on the shear surface

τ_2 = shear strength of concrete (The value for the shear strength of concrete was taken as the standard tensile strength of concrete f_{tk}, according to the research of Hofbeck et al.[20] and Zhang and Guo.[21] In this paper, 2.39 MPa [347 psi] was used for the value of f_{tk} because the concrete strength of the PRPs and the cast-in-place concrete topping was C40, according to China's *Code for Design of Concrete Structures*.[17])

A_2 = area of the normal concrete shear surface (the area where the cast-in-place concrete passing through the rectangular hole of the ribs is cut for shear surface 1 or the area where the ribs are cut for shear surface 2) (Fig. 9)

A = horizontal projection area of the shear surface

The contribution of the transverse reinforcement to the shear resistance is not included in Eq. (3) because the reinforcing bars across the shear surface do not have a significant shear effect until the bond between the cast-in-place and precast concrete at the interface has been destroyed.

Shear stress on the combined interface The size of the CSPRP in this study was 6000 × 3600 × 120 mm (141.7 × 236.2 × 4.7 in.) with a span-to-depth ratio of 0.033, which belongs to the thin-plate category. The reinforcement of the CSPRP was different in each direction, and the slab can be regarded as an orthotropic plate. The shear stress on the combined interface of CSPRPs under load can be estimated using the theory of elastic thin plates. In this paper, the boundary conditions of the specimens are simplified by considering three edges to be simply supported and one edge fixed. (The intermediate support of the two-span continuous slab can be regarded as the fixed end of a single-span slab.) A single span was used for the analysis (**Fig. 10**), which is appropriate according to the symmetry principle. The dashed lines in Fig. 10 indicate the simply supported boundary condition. The elastic curved surface differential equation[22] for the plate is

$$B_x \frac{\delta^4 \omega}{\delta x^4} + 2B \frac{\delta^4 \omega}{\delta x^2 \delta y^2} + B_y \frac{\delta^4 \omega}{\delta y^4} = q \qquad (4)$$

where

B_x = bending stiffness in the x direction

ω = vertical deflection outside the plate plane

x = location on the plate measured along the x axis

B = effective torsional stiffness of the orthotropic plate

  = $\sqrt{B_x B_y}$ for a reinforced concrete slab with constant thickness

y = location on the plate measured along the y axis

B_y = bending stiffness in the y direction (prestressed direction)

q = uniform load acting on the plate

Equation (4) can be solved using the Levy method, and the single trigonometric series.

$$\omega = \sum_{m=1}^{\infty} Y_m \sin \frac{m\pi x}{a}$$

where

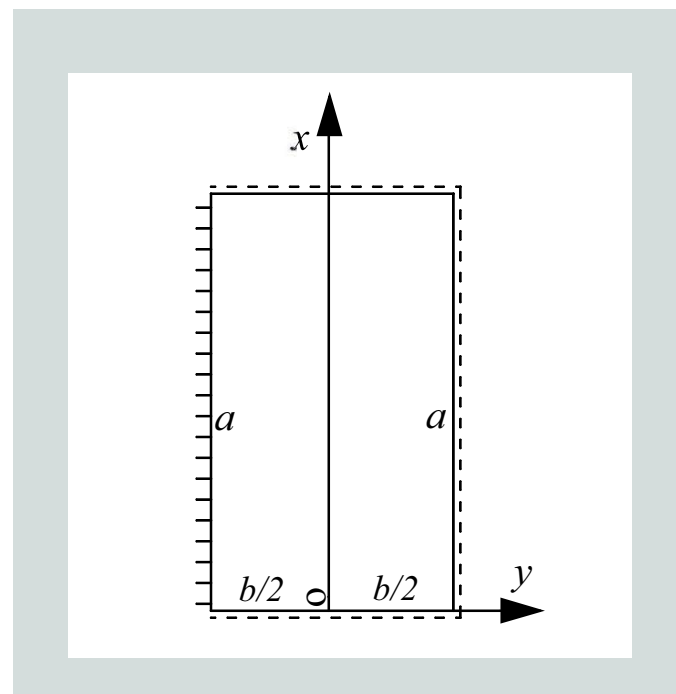m = any positive integer

Y_m = a function of y

a = length of the slab

Figure 10. Calculation diagram of the CSPRP. Note: *a* = length of slab; *b* = width of slab; CSPRP = composite slab with precast concrete ribbed panels; *x* = location measured along the x axis; *y* = location measured along the y axis.

The solution to Eq. (4) can be obtained using Eq. (5).

$$\omega = \sum_{m=1,3,5}^{\infty} \left[\left(A_m + B_m y\right)\cosh\left(\frac{m\pi\lambda}{a}y\right) \right.$$
$$\left. + \left(C_m + D_m y\right)\sinh\left(\frac{m\pi\lambda}{a}y\right) + \frac{4qa^4}{m^5\pi^5 B_x} \right]\sin\frac{m\pi x}{a} \qquad (5)$$

where

A_m, B_m, C_m, and D_m = differential equation coefficients to be solved for based on the boundary conditions

There are four boundary conditions to be applied for the solution.

At the simply supported edges, the deflection and bending moment are zero:

λ = a coefficient relating to the bending stiffness of orthotropic slabs in the orthogonal direction = $\sqrt[4]{\dfrac{B_x}{B_y}}$

$$\omega\big|_{y=\frac{b}{2}} = 0$$

and

$$\delta^2\omega/\delta y^2 + 0.2\delta^2\omega/\delta x^2\big|_{y=\frac{b}{2}} = 0$$

At the fixed edge, the deflection and rotation are zero.

$$\omega\big|_{y=-\frac{b}{2}} = 0$$

and

$$\delta\omega/\delta y\big|_{y=-\frac{b}{2}} = 0$$

where

b = width of the slab

The four coefficients in Eq. (5) can be obtained by applying the four boundary conditions.

$$A_m = \left\{ a^3q\left[-11abm\pi\lambda\cosh\left(\frac{bm\pi\lambda}{2a}\right) + 3abm\pi\lambda\cosh\left(\frac{3bm\pi\lambda}{2a}\right) \right.\right.$$
$$\left.\left. + 2\left(-b^2m^2\pi^2\lambda^2 + 8a^2\cosh\left\{\frac{bm\pi\lambda}{a}\right\}\right)\sinh\left(\frac{bm\pi\lambda}{2a}\right)\right]\right\}$$
$$\bigg/ \left\{ m^5\pi^5\left[2bm\pi\lambda - a\sinh\left(\frac{2bm\pi\lambda}{a}\right)\right]B_x \right\}$$

$$B_m = \frac{4a^3q\lambda\sinh\left(\frac{bm\pi\lambda}{2a}\right)\left[-bm\pi\lambda + a\sinh\left(\frac{bm\pi\lambda}{a}\right)\right]}{m^4\pi^4\left[-2bm\pi\lambda + a\sinh\left(\frac{2bm\pi\lambda}{a}\right)\right]B_x}$$

$$C_m = \frac{2a^3bq\lambda\cosh\left(\frac{bm\pi\lambda}{2a}\right)\left[-bm\pi\lambda + a\sinh\left(\frac{bm\pi\lambda}{a}\right)\right]}{m^4\pi^4\left[-2bm\pi\lambda + a\sinh\left(\frac{2bm\pi\lambda}{a}\right)\right]B_x}$$

$$D_m = \frac{2a^3q\lambda\left[2bm\pi\lambda\cosh\left(\frac{bm\pi\lambda}{2a}\right) + 5a\sinh\left(\frac{bm\pi\lambda}{2a}\right) - 3a\sinh\left(\frac{bm\pi\lambda}{2a}\right)\right]}{m^4\pi^4\left[2bm\pi\lambda - a\sinh\left(\frac{2bm\pi\lambda}{a}\right)\right]B_x}$$

The stress-resultant τ_0 of interlayer shear stress τ_{xz} and τ_{yz} is the main factor that influences the delamination of composite slabs. The expressions for interlayer shear stress[22] are

$$\tau_{xz} = -\left(\frac{3}{2\delta} - \frac{6z^2}{\delta^3}\right)\frac{\delta}{\delta x}\left(B_x\frac{\delta^2\omega}{\delta x^2} + B\frac{\delta^2\omega}{\delta y^2}\right)$$

$$\tau_{yz} = -\left(\frac{3}{2\delta} - \frac{6z^2}{\delta^3}\right)\frac{\partial}{\partial y}\left(B_y\frac{\delta^2\omega}{\delta y^2} + B\frac{\delta^2\omega}{\delta x^2}\right)$$

$$\tau_0 = \sqrt{\tau_{xz}^2 + \tau_{yz}^2} \qquad (6)$$

where

z = vertical distance from the calculated surface to the neutral plane of the slab

In this paper, z is 30 mm (1.18 in) because the thickness of the CSPRP and PRPs was 120 mm (4.72 in.) and 30 mm, respectively.

Composite slabs that use PRPs as the load-bearing structure and formwork are secondary load slabs and are generally constructed without falsework, which means no shear stress occurs on the combined interface under self-weight. Under the experimental conditions in this paper, the maximum shear stress on the combined interface calculated by Eq. (5) is at the center of the long fixed edge. The shear stress on the combined interface τ_0 was 0.13 MPa (19 psi) without considering self-weight and 0.20 MPa (29 psi) considering self-weight, and in both cases the permanent dead load and live load acting on the upper surface of the CSPRP were 2.0 kN/m² (0.29 psi) and 4.0 kN/m² (0.58 psi), respectively. Zhu et al.[23] conducted a finite element analysis of a composite slab with a span of 3300 mm (129.9 in.) and a thickness of 120 mm (4.72 in.), and the maximum shear stress on the combined interface was 0.373 MPa (54.1 psi) under a uniform load. In addition, Wang and Guo[24] noted that the shear stress in the slabs used in buildings is about 0.2 to 0.3 MPa (29 to 43.5 psi). Thus, it is reasonable to use 0.4 MPa (58 psi) as the upper limit for the shear stress on the combined interface of composite slabs for typical loads and spans.

Table 4 shows the shear requirements and shear capacity of CSPRPs and common flat-plate composite slabs for typical loads, spans, and constraints. Table 4 shows that the shear

behavior on the combined interface of the CSPRP can meet shear requirements under serviceable working conditions better than common flat-plate composite slabs. Common flat-plate composite slabs can also meet the shear requirement on the combined interface under serviceable working conditions even if they are used as floor slabs.

Tensile stress on the combined interface The combined interface of a CSPRP is also a weak tensile surface. When extreme stress was applied to the combined surface (Fig. 4), satisfactory composite action was observed until loading was stopped. This finding indicates that the bonding tensile strength between PRPs and cast-in-place concrete toppings is adequate even when they are working together under the combined action of tensile stress and shear stress. In fact, although the bottom of the CSPRP is typically connected to a suspended ceiling in working conditions, the weight of the suspended ceiling is small compared with the 14.49 kN/m^2 (2.1 psi) load applied in this study. Thus, the bonding tensile strength on the combined interface of CSPRPs can meet its tensile resistance requirements under serviceable working conditions and the combined interface will not be disengaged.

Conclusion

Out-of-plane static loading tests of a CSPRP and a comparable cast-in-place slab were conducted using a hanging load. The following conclusions are based on the analysis in this paper:

- Compared with the traditional method of loading composite slabs, which consists of distributing the load on the top surface, the hanging load method enabled the study of the out-of-plane integrity of composite slabs under the least favorable stress conditions.

- The stiffness and crack resistance of the CSPRP and cast-in-place slab were observed to be similar, though the cracking patterns were different. At the 0.1 mm (0.004 in.) crack control level, the flexural capacity of the CSPRP is higher than that of the cast-in-place concrete slab.

- The presence of ribs with regularly distributed rectangular holes increases the average shear strength of the combined interface. As a result, the average shear strength of CSPRPs available to meet shear requirements is greater than the average shear strength of common flat-plate composite slabs. The combined interface will not disengage under serviceable working conditions.

Acknowledgments

References

1. Yee, A. A. 2001. "Structural and Economic Benefits of Precast/Prestressed Concrete Construction." *PCI Journal* 46 (4): 34–43.

2. Yee, A. A. 2001. "Social and Environmental Benefits of Precast Concrete Technology." *PCI Journal* 46 (3): 14–19.

3. Baran, E. 2015. "Effects of Cast-in-Place Concrete Topping on Flexural Response of Precast Concrete Hollow-Core Slabs." *Engineering Structures* 98: 109–117.

4. Scott, N. L. 1973. "Performance of Precast Prestressed Hollow Core Slab with Composite Concrete Topping." *PCI Journal* 18 (2): 64–77.

5. Adawi, A., M. A. Youssef, and M. E. Meshaly. 2015. "Experimental Investigation of the Composite Action between Hollowcore Slabs with Machine-Cast Finish and Concrete Topping." *Engineering Structures* 91: 1–15.

6. Kumar, N. V., and J. A. Ramirez. 1996. "Interface Horizontal Shear Strength in Composite Decks with Precast Concrete Panels." *PCI Journal* 41 (1): 42–55.

7. Tang, L., Z. X. Go, and G. P. Ding. 2013. "Structural Performance Test Research on the New Steel Bar Truss Concrete Superimposed Two-Way Slab." [In Chinese.] *Industrial Construction* 43 (11): 49–53.

8. Li, J., P. F. Huang, Y. Y. Chen, et al. 2013. "Experimental Research on Mechanical Properties of Self-Sustaining Steel Bar Truss and Concrete Superposed Slab." [In Chinese.] *Structural Engineers* 29 (4): 132–139.

9. An, H. Y., L. Jia, and Y. J. Ding. 2012. "Experimental Research on Mechanical Performance of Two-Way Prestressed Laminated Concrete Slab and Its Application." [In Chinese.] *Building Structure* 42 (12): 90–93.

10. Wu, F. B., H. L. Huang, W. Chen, et al. 2011. "Experimental Study and Calculating Method on Bending Rigidity of Precast Prestressed Concrete Ribbed Panels for Composite Slabs." [In Chinese.] *Journal of Hunan University (Natural Sciences)* 38 (4): 1–7.

11. Zhang, J. S., Y. Yao, X. H. Zhou, et al. 2013. "Failure Mode and Ultimate Bearing Capacity of Precast Ribbed Panels Used for Concrete Composite Slabs." *Advances in Structural Engineering* 16 (12): 2005–2017.

12. Zhang, J. S., Y. Z. Wang, Y. Yao, et al. 2016. "Influence of Reinforcement on In-Plane Mechanical Behaviors of CSPRP under Cyclic Reversed Load." *Materials and Structures* 49 (1–2): 101–116.

13. Zhang, J. S., Y. S. Ni, Y. Yao, et al. 2015. "In-Plane Mechanical Property of Superimposed Concrete Slab with Precast Ribbed Panels Jointed in Different Directions." [In Chinese.] *China Civil Engineering Journal* 5: 23–34.

14. Wu, F. B., B. Liu, X. H. Zhou, et al. 2014. "Analysis of the Interlocking Effect of the Combined Interface in a New Type of Composite Floor." [In Chinese.] *Journal of Hunan University (Natural Sciences)* 41 (2): 1–7.

15. Wu, F. B., L. B. Deng, B. Liu, et al. 2014. "Experimental Study on Four-Sides Simply Supported Single-Direction-Prestress Double-Direction-Tendon Concrete Composite Floorslab." [In Chinese.] *Building Structure* 44 (5): 6–11.

16. Yao, Y., J. S. Zhang, J. Liu, et al. 2014. "Technical Characteristics and Economic Comparison of Concrete Composite Slab with Precast Ribbed Bottom Panel." [In Chinese.] *Architecture Technology* 45 (1): 77–79.

17. Ministry of Housing and Urban-Rural Construction of the People's Republic of China. 2010. *Code for Design of Concrete Structures*. [In Chinese.] GB 50010-2010. Beijing, China: China Architecture and Building Press.

18. China Academy of Building Research. 2012. *Standard Method for Testing of Concrete Structure*. [In Chinese.] GB 50152-2012. Beijing, China: China Architecture and Building Press.

19. Guo, J. J., S. B. Wang, L. S. Zhang, et al. 2002. "Experimental Research for the Behavior of Bond between New and Old Concrete." [In Chinese.] *Building Structure* 32 (8): 43–45.

20. Hofbeck, J. A., I. O. Ibrahim, and A. H. Mattock. 1969. "Shear Transfer in Reinforced Concrete." *Journal of the American Concrete Institute* 66 (2): 119–128.

21. Zhang, Q., and Z. H. Guo. 1992. "Investigation on Shear Strength and Shear Strain of Concrete." [In Chinese.] *Journal of Building Structures* 13 (5): 17–24.

22. Timoshenko, S. P., and S. Woinowsky-Krieger. 1959. *Theory of Plates and Shells*. New York, NY: Mc-Graw-Hill.

23. Zhu, Z. F., Z. X. Guo, and L. Tang. 2015. "Mechanical Behavior Analysis of Prestressed Concrete Composite Slab." [In Chinese.] *World Earthquake Engineering* 31 (4): 280–284.

24. Wang, S. H., and Y. C. Guo. 1986. "Design and Application of Prestressed Composite Slab without Binding Bar." [In Chinese.] *Architecture Technology* 8: 48–50.

Notation

a = length of the slab

A = horizontal projection area of the shear surface

A_1 = area of bonded surface between the cast-in-place and precast concrete on the shear surface

A_2 = area of the normal concrete shear surface (the area where the cast-in-place concrete passing through the rectangular hole of the ribs is cut for shear surface 1 or the area where the ribs are cut for shear surface 2)

A_m = differential equation coefficient to be solved for based on the boundary conditions

A_p = area of single prestressed wire used for the longitudinal reinforcement in the short-span direction of specimen DH

A_s = area of single reinforcing bar used for the longitudinal reinforcement in the short-span direction of specimen XJ

b = width of the slab

B = effective torsional stiffness of the orthotropic plate

B_m = differential equation coefficient to be solved for based on the boundary conditions

B_x = bending stiffness in the x direction

B_y = bending stiffness in the y direction (prestressed direction)

C_m = differential equation coefficient to be solved for based on the boundary conditions

d = spacing of the longitudinal reinforcement in the short-span direction of specimen XJ

d_1 = spacing of the prestressed wires of specimen DH

D_m = differential equation coefficient to be solved for based on the boundary conditions

f_c = average value of measured concrete compressive strength

f_{pu} = measured average ultimate tensile strength of prestressed wire used for the longitudinal reinforcement in the short-span direction of specimen DH

f_{su} = measured average ultimate tensile strength of reinforcing bar used for the longitudinal reinforcement in the short-span direction of specimen XJ

f_{tk} = standard tensile strength of concrete

f_u = average value of measured ultimate tensile strength

f_y = average value of measured yield tensile strength

h = thickness of specimens XJ and DH

m = any positive integer

q = uniform load acting on the plate

x = location on the plate measured along the x axis

y = location on the plate measured along the y axis

Y_m = function of y

z = vertical distance from the calculated surface to the neutral plane of the slab

δ = thickness of the slab

λ = a coefficient relating to the bending stiffness of orthotropic slabs in the orthogonal direction = $\sqrt[4]{\dfrac{B_x}{B_y}}$

τ = average shear strength of the combined interface

τ_0 = stress resultant of interlayer shear stress τ_{xz} and τ_{yz}

τ_1 = shear strength of the bond between the cast-in-place and precast concrete

τ_2 = shear strength of concrete

τ_{xz}, τ_{yz} = interlayer shear stress

ω = vertical out-of-plane deflection of the plate

About the authors

Jingshu Zhang, PhD, is a professor at the Key Laboratory of Mechanics on Disaster and Environment in Western China of the Ministry of Education at Lanzhou University in Lanzhou, China, and a professor at the School of Civil Engineering and Mechanics at Lanzhou University.

Binyang Liu is an engineer at CISDI Engineering Co. Ltd. in Chongqing, China. Liu was a master's degree candidate at the Key Laboratory of Mechanics on Disaster and Environment in Western China of the Ministry of Education at Lanzhou University in Lanzhou, China, and a master's degree candidate in the School of Civil Engineering and Mechanics at Lanzhou University.

Binbin Han is an engineer at Tianshui Architecture Design Group in Gansu, China. Han was a master's degree candidate at the Key Laboratory of Mechanics on Disaster and Environment in Western China of the Ministry of Education at Lanzhou University and a master's degree candidate in the School of Civil Engineering and Mechanics at Lanzhou University.

Yongsong Ni is an engineer at the China Architecture Design and Research Group in Beijing, China. Ni was a master's degree candidate at the Key Laboratory of Mechanics on Disaster and Environment in Western China of the Ministry of Education at Lanzhou University and a master's degree candidate at School of Civil Engineering and Mechanics at Lanzhou University.

Zhenlong Li is an engineer at the Administrative Examination and Approval Bureau of Chongli District in Zhangjiakou, Heibei, China. Li was a master's degree candidate at the Key Laboratory of Mechanics on Disaster and Environment in Western China of the Ministry of Education at Lanzhou University and a master's degree candidate in the School of Civil Engineering and Mechanics at Lanzhou University.

Abstract

When studying the out-of-plane performance of a composite slab, distributing the load on the top slab surface may overestimate the integrity of the combined interface and result in unsafe shear capacity because the load path is from the top surface to the bottom of the slab. It is difficult to observe cracking and crack distribution on the top surface of the slab during load application. In this paper, a static hanging load test of a two-span, two-way composite slab with precast concrete ribbed panels (CSPRP) was conducted. The hanging loading conditions were achieved by constructing loading frames and connecting the frames to a series of inverted U-shaped cables, which were suspended from the ribs of the precast concrete ribbed panels.

After the cast-in-place concrete topping achieved its design strength, concrete blocks were placed in the loading frame to load the CSPRP. A comparative test of a two-span, two-way cast-in-place concrete slab was conducted at the same time, under the same conditions. The results showed that CSPRPs and cast-in-place concrete slabs exhibited comparable performance. The stiffness and crack resistance of CSPRPs were similar to those of cast-in-place concrete slabs. The mechanical properties of the combined interface of the CSPRP was compared with a common flat-plate composite slab. The results showed that the shear behavior on the combined interface of CSPRPs meets the shear strength requirements under serviceable working conditions better than common flat-plate composite slabs. The combined interface of CSPRPs will not disengage under service loads.

Keywords

Review policy

Reader comments